Stopping Transformed Growth with Cytoskeletal Proteins: Turning a Devil into an Angel

Bo Yang [1], Haguy Wolfenson [2,3], Naotaka Nakazawa [1], Shuaimin Liu [4], Junqiang Hu [4], Michael P. Sheetz [1,2,*]

[1]Mechanobiology Institute, National University of Singapore, Singapore 117411.

[2]Department of Biological Sciences, Columbia University, New York, NY 10027.

[3]Current address: Department of Genetics and Developmental Biology, The Ruth and Bruce Rappaport Faculty of Medicine, The Technion-Israel of Technology, Haifa, Israel 31096.

[4]Department of Mechanical Engineering, Columbia University, New York, NY 10027.

*Correspondence: ms2001@columbia.edu

Summary

A major hallmark of cancer is uncontrolled growth on soft matrices, i.e. transformed growth. Recent studies show that local contractions by cytoskeletal rigidity sensor units block growth on soft surfaces and their depletion causes transformed growth. The contractile system involves many cytoskeletal proteins that must be correctly assembled for proper rigidity sensing. We tested the hypothesis that cancer cells lack rigidity sensing due to their inability to assemble contractile units because of altered cytoskeletal protein levels. In four widely different cancers, there were over ten-fold fewer rigidity-sensing contractions compared with normal fibroblasts. Restoring normal levels of cytoskeletal proteins restored rigidity sensing and rigidity-dependent growth in cancer cells. Most commonly, this involved restoring balanced levels of the tropomyosins 2.1 (often depleted by miR-21) and 3 (often overexpressed). Restored cells could be transformed again by depleting other cytoskeletal proteins including myosin IIA. Thus, the depletion of rigidity sensing modules enables growth on soft surfaces and many different perturbations of cytoskeletal proteins can disrupt rigidity sensing thereby enabling transformed growth.

Introduction

For normal cell growth, complex cellular mechanical functions sense the microenvironment. When cells encounter the wrong environment, the output from these sensing events will block growth. Matrix rigidity is an important aspect of the microenvironment for normal development and regeneration, whereas cancer cells ignore rigidity and grow on very soft surfaces. This is the basis for the soft agar assay, which is a standard test for the malignancy level of cancers (*1*). We recently described the rigidity sensing apparatus as a cytoskeletal protein complex that contracts matrix to a fixed distance; if the force generated by this contraction exceeds about 25 pN, the matrix will be considered rigid (*2*). This is just one of a number of modular machines that perform important tasks in cells similar to the clathrin-dependent endocytosis complex (*3*). Such machines typically assemble rapidly from mobile components, perform the desired task and disassemble in a matter of seconds to minutes. They are activated by one set of signals and are designed to generate another set of signals. The cell rigidity sensing complex is a 2-3 μm-sized modular machine that forms at the cell periphery during early contact with matrix (*2, 4-7*). It is powered by sarcomere-like contractile units (CUs) that contain myosin-IIA, actin filaments, tropomyosin 2.1 (Tpm 2.1), α-actinin 4, and other cytoskeletal proteins (*7*). The number of CUs depends upon EGFR or HER2 activity as well as substrate rigidity (*6*). Further, the correct length and duration of contractions are controlled by receptor tyrosine kinases through interactions with cytoskeletal proteins (*5*). CUs are activated in spreading cells; and on rigid surfaces, they stimulate the formation of mature adhesions. However, on soft surfaces, contractions are very short-lived and adhesions rapidly disassemble, leading to cell death by *anoikis* (*2, 7*). Since cancer cells fail to activate *anoikis* pathways on soft matrices, we hypothesize that rigidity-sensing CUs can block growth on soft surfaces and their depletion in cancer cells can enable growth on soft agar.

Cytoskeletal proteins are highly integrated and their functions are well studied in normal cells (*8*). However, the role of cytoskeletal components in cell transformation and cancer metastasis development is still not clear. Mutations and abnormal expression of various cytoskeletal or cytoskeletal-associated proteins have been reported in many cancer studies (*9*): Myosin IIA has been identified as a tumor suppressor of squamous cell carcinomas (*10*); The expression level of Tpm 2.1, one isoform from the tropomyosin family, is highly suppressed in a variety of cancer cell lines (*11*); Tpm 3, another tropomyosin isoform, has been reported to be the predominant tropomyosin in primary tumors and tumor cell lines (*12*). Interestingly, in studies using arrays of elastic PDMS pillars, depletion of Tpm 2.1 in normal MCF 10A cells caused transformation as well as disruption of CU formation, while restoration of normal levels of Tpm 2.1 in metastatic MDA-MB-231 cells blocked transformed growth on soft agar (*2, 11*). Further, removing another CU component, α-actinin 4, in mouse embryonic fibroblast (MEF) cells enabled rapid growth on soft matrices (*7*). These findings indicated that unbalanced expression levels of different cytoskeletal proteins correlates with cell transformation. Here we extend those findings to show that widely different cancer lines do not have rigidity-sensing contractions and that modifications of cytoskeletal protein levels can restore contractions along with the activation of apoptosis on soft surfaces.

Results:

Transformed cells lack rigidity sensing activity due to altered levels of contractile unit (CU) components.

To examine the relationship between rigidity sensing CU formation and transformed growth, we examined four different cancer lines and a transformed cell line, each randomly selected from a different tissue. The bases of transformation are listed for each line in Table 1: 1) Cos7 cells were derived from African green monkey kidney fibroblast cells by SV40 transformation; 2) MDA-MB-231 human breast cancer line formed tumors in nude mice (*13, 14*); 3) HT1080, a fibrosarcoma line from an untreated patient that carried an IDH1 mutation (*15*); 4) SKOV3 a human ovarian adenocarcinoma line with an epithelial-like morphology (*16*); 5) LLC, a lung carcinoma line from a C57BL mouse (*17*). Human foreskin fibroblast (HFF) cells served as the non-transformed control. CU activity was measured by a previously described method (*6*) that involved spreading cells on arrays of elastic pillars (0.5 μm diameter) and automated analyses of the pillar displacements (see displacements of two nearby pillars toward each other (a CU) at the cell periphery in Supplementary Figure 1). Consistent with previous publications, HFF cells generated 145±14.3 CUs on rigid pillars (k=8.4 pN/nm) and 66±3.7 CUs on soft pillars (k=1.6 pN/nm) per 10 minutes during the first 30 minutes of spreading. In contrast, all the transformed cells produced no or few CUs (less than 10) on the two pillar types during early spreading (Figure 1 A and B). To test whether cells were able to distinguish between rigid and soft surfaces at a later spreading stage, we plated the 6 different cell lines on stiff (2MPa) and compliant (5kPa) fibronectin-coated PDMS surfaces for 6 hours. Cells were then fixed and stained with paxillin and actin as markers for adhesion formation and morphology change, respectively (Figure 1 C). As previously described (*18*), HFF cells polarized on rigid PDMS and spread less on soft PDMS in a round shape. However, all the five transformed cell lines showed no significant difference in cell polarization level or adhesion size on the surfaces with a 400-fold difference in rigidity (Figure 1 D and E). Since transformation was defined classically as growth on soft agar (*1*), we cultured the

different cell lines in soft agar for 7 days. All five transformed cell lines formed colonies while HFF cells barely survived (Figure 1 F and G). Thus, none of the transformed lines developed a significant number of CUs for rigidity sensing. This was consistent with the inability of those lines to react to differences in matrix rigidity and to grow on soft surfaces.

Why did the transformed cells lines lack rigidity sensing activity? To answer this question, we performed western blot analyses of the known CU proteins (Figure 2 A), including kinases (EGFR, HER2, and ROR2) and cytoskeletal proteins (Myosin IIA, Tpm 2.1 and Tpm 3) (Figure 2 B). To our surprise, the protein levels of selected cytoskeletal proteins followed a similar trend in different transformed cells. Both myosin IIA and Tpm 2.1 levels were suppressed, while Tpm 3 expression level was increased in most cancer lines. On the other hand, the pattern of RTK levels varied from cell line to cell line (Figure 2 C). Thus, different patterns of depletion of cytoskeletal components in transformed cells correlated with the loss of CUs, which raised the questions: 1) Could CUs be restored by restoring normal levels of those missing components? 2) Would depletion of another CU protein in restored cells inhibit CU formation and again cause transformed growth?

Restoration of missing cytoskeletal proteins enables CU formation and rigidity sensing in transformed cells.

To address these questions we first tested whether we could block transformed growth by simply restoring the missing CU components for rigidity sensing. We selected Cos7 cells, which lacked myosin IIA, as the first candidate. After expression of EGFP-myosin IIA, Cos7 cells generated CUs on both soft and rigid pillar surfaces (Figure 3 C and D) (107 CUs/cell were observed on rigid

pillars and 45 CUs/cell on soft pillars in 10 mins); whereas untransfected cells produced occasional large, unpaired contractions of soft pillars (Figure 3 A and B). In addition, after 6 hours of spreading, Cos7 cells normally formed tiny focal adhesions of similar size on both soft (0.58±0.08 μm^2) and rigid (0.54±0.05 μm^2) flat PDMS surfaces (Figure 3 E). However, after myosin IIA expression, Cos7 cells generated larger focal adhesions (1.03±0.1 μm^2) on rigid and smaller adhesions (0.65±0.03 μm^2) on soft surfaces as commonly observed for normal fibroblast cell lines (Figure 3 F and G). We then tested for colony growth of wild type Cos7 cells and Cos7-IIA cells on soft agar. Cos7-IIA cells did not survive after 7 days in culture whereas control Cos7 cells proliferated and formed colonies (Supplementary Figure 2).

To further prove that restoration of rigidity sensing activity in Cos7 cells was caused by myosin IIA and not by increasing the total amount of myosin in the cells, we next transfected myosin IIB in cos7 cells. The Cos7-myosin IIB cells did not generate any CUs on pillar surfaces during initial spreading and they formed focal adhesions of similar size on both rigid (0.31±0.05 μm^2) and soft (0.35±0.03 μm^2) fibronectin-coated PDMS 6 hours after plating (Supplementary Figure 3 A and B). Thus, the re-expression of myosin IIA but not myosin IIB in Cos7 cells restored rigidity-sensing activity and blocked transformed growth.

To investigate whether this connection between CU formation and transformed growth was cell line dependent, we next examined a highly metastatic human breast cancer cell line that formed aggressive tumors in nude mice and was depleted of Tpm 2.1, MDA-MB-231 cells (*13*). Consistent with previous studies (*2*), restoration of Tpm 2.1 in MDA-MB-231 cells restored CUs (76±6 CUs per 10 mins per cell on rigid pillars) (Supplementary Figure 4 A and B). The other cell line that

was missing Tpm 2.1 was SKOV3 and restoration of normal levels of Tpm 2.1 in those cells restored CUs as well (data not shown). The Tpm 2.1 transfected MDA-MB-231 cells (231-Tpm) distinguished between soft and rigid PDMS by generating larger focal adhesions and spreading to larger areas on rigid (Supplementary Figure 4 C and D). Further, control MDA-MB-231 but not 231-Tpm cells formed colonies in soft agar culture after 7 days (Supplementary Figure 4 E).

Reciprocal depletion of other cytoskeletal CU components restored transformed growth and blocked CU formation

Because Cos7 cells differed greatly from MDA-MB-231 cells, we next asked whether reciprocal depletion of Tpm 2.1 and myosin-IIA could restore the transformed phenotype in Cos7-IIA and 231-Tpm cells, respectively. Previously, depletion of Tpm 2.1 caused transformed growth in MCF-10A cells (*2*). Upon siRNA depletion of endogenous Tpm 2.1 (Figure 4 A), CU formation in Cos7-IIA cells was dramatically decreased (7±1.3 CUs on rigid and 3.4 ±1 CUs on soft pillars) (Figure 4 C). Despite the lack of CUs, Tpm2.1-depleted Cos7-IIA cells produced larger displacements on both soft and rigid pillars, showing that myosin-IIA was still active (Figure 4 B). Moreover, consistent with previous studies of MEF cells (*2*), depletion of Tpm2.1 in Cos7-IIA cells caused a significant decrease of FA size on glass surfaces (Supplementary Figure 5 A-C). Further, Tpm 2.1-depleted Cos7-IIA cells survived on 2.3 kPa PAA gels without activating Caspase-3 cleavage (Supplementary figure 5 D and E). In the soft agar assay, visible colonies of Tpm 2.1-depleted Cos7-IIA cells formed (Figure 4 D and E). Thus, depletion of Tpm2.1 in Cos7-IIA cells blocked CU formation and restored transformed growth.

In a reciprocal manner, depletion of endogenous myosin-IIA in 231-Tpm cells (Figure 4 F) inhibited CU formation on both rigid and soft pillars by 4-fold and decreased overall contractility (Figure 4 G and H). In addition, the myosin-IIA-depleted 231-Tpm cells showed a disruption of stress fibers and also a significant reduction of focal adhesion size on glass (Supplementary Figure 6 A-C). Further, myosin-IIA-depleted 231-Tpm cells grew as well as wild type 231 cells on soft surfaces and the expression level of cleaved-Caspase-3 on soft surfaces also decreased 2-fold (Supplementary Figure 6 D and E). Additionally, after myosin-IIA silencing, 231-Tpm cells formed colonies on soft agar similar to MDA-MB-231 cells after 7 days (Figure 4 I and J). Thus, in the restored cell lines, depletion of other CU components blocked CU formation and induced transformed cell growth. This indicated that rigidity sensing CU formation blocked anchorage-independent growth and loss of rigidity sensing enabled transformed growth. Further, this was robust in widely different cell backgrounds (Figure 4 K).

A low molecular weight tropomyosin, Tpm 3, suppressed CU formation

Careful examination of the western blot screening data (Figure 2 B) raised a question about why HT1080 cells failed to generate CUs for rigidity sensing despite expressing the needed CU components. It was noted that they also had high levels of another tropomyosin, Tpm 3, which was highly expressed in most cancer cells (*12*). To determine if Tpm 3 may suppress CU formation, we silenced the endogenous Tpm 3 in HT1080 cells by siRNA (Figure 5 A). As shown in Figure 5 B, the Tpm 3-depleted HT1080 cells generated 50±8 CUs on rigid pillars and 35±5 CUs on soft pillars, approximately 2-fold higher than control HT1080 cells. Moreover, the depletion of Tpm 3 or inhibition of Tpm 3 assembly on actin filaments by TR100 or ATM 3507 (12) decreased the

size and number of colonies that HT1080 cells formed in soft agar after 7-days culturing (Figure 5 E). Thus, these results supported the idea that the high level of Tpm 3 protein in transformed cells suppressed CU formation and stimulated transformed growth (Figure 5 F).

To check if knocking down Tpm 3 by siRNA would activate CU formation even in the absence of Tpm 2.1, we knocked down Tpm 3 in MDA-MB-231 cells (Figure 5 C) that lacked endogenous Tpm 2.1. Tpm 3 knock down failed to increase the total number of CUs when compared with the control group (Figure 5 D). This indicated that Tpm 2.1 expression was necessary for CU formation and cell rigidity sensing (Figure 5 F).

Decreased expression of high molecular weight tropomyosins (including Tpm 2.1) and increased expression of low molecular weight tropomyosins (including Tpm 3) were reported in cells transformed by various oncogenes, carcinogens and viruses (*19*). The relationship between Tpm 2.1 and Tpm 3 in CU formation and cell rigidity sensing regulation was complicated. Since silencing Tpm 3 in Tpm 2.1-expressing transformed cells increased the number of CUs formed during early spreading, there appeared to be a competition between Tpm 2.1 and Tpm 3 during CU formation. To test this hypothesis, we next asked the question of whether overexpressing Tpm 3 in a normal fibroblast cell line would suppress cell rigidity sensing. To that end, HFF cells expressing high levels of EGFP-Tpm 3 were analyzed on pillar surfaces. The total number of CUs in these cells was significantly lower than in the wild-type HFF cells on both rigid and soft pillars (Figure 5 G and H). This indicated that high expression levels of Tpm 3 inhibited CU formation, potentially through competing with Tpm 2.1 (Figure 5 I).

To further examine the behavior of Tpm 2.1 in the Tpm 3-overexpressing cells, we fixed and stained the endogenous Tpm 2.1 in HFFs with or without Tpm 3 overexpression after 15 mins spreading on pillars. Consistent with previous observations (*2*), Tpm 2.1 concentrated at cell edges in control HFFs. However, this peripheral localization of Tpm 2.1 disappeared in Tpm 3 overexpressed cells (Supplementary figure 7). Thus, high levels of Tpm 3 inhibited cell rigidity sensing CU formation by competing with endogenous Tpm 2.1 in normal fibroblasts.

Discussion

Based upon the current and related findings, transformation follows upon the unbalanced expression of different cytoskeletal proteins that decreases rigidity sensing contractile unit (CU) formation in all tested cell lines. In many different cell backgrounds, CUs are needed for rigidity-dependent growth, i.e., growth on rigid surfaces and activation of Caspase-3-dependent *anoikis* on soft matrices. In the initial characterization of CUs, the major cytoskeletal components, Tpm 2.1, myosin-IIA, and α-actinin 4, are necessary components for CU formation (*2, 7*). In these studies, overexpression of another cytoskeletal protein, Tpm 3, causes CU disruption. Interestingly, all of these components are either tumor suppressors (Tpm 2.1, Myosin IIA and a-actinin 4) or tumor promoters (Tpm 3). From previous studies, Tpm 2.1 is down-regulated in a wide variety of transformed cell lines (*20-23*). Overexpression of miR-21, a microRNA that targets the Tpm 2.1 RNA (*24*), is observed in breast tumors and correlates with the severity of the disease (*25*). Further, reduction of miR-21 induces glioma cell apoptosis through Caspase pathways (*26*). In an *in vivo* RNAi screen, myosin-IIA has been identified as a tumor suppressor of squamous cell carcinomas (*10*). α-actinin 4, as well, has been recognized as a tumor suppressor in cases of neuroblastoma

and lung cancers (*27, 28*). In contrast, Tpm 3 is responsible for metastatic melanoma motility regulation (*29*) and expression levels are elevated in many different cancer lines (*12*). Thus, cancer cells that are characterized by transformed growth on soft surfaces, have altered levels of various cytoskeletal proteins that correlate with the loss of local CUs involved in rigidity sensing.

One of the major pathways to induce transformation is to express mutant Ras, which is normally activated by a variety of RTKs that participate in cell proliferation, transformation, and regulation of differentiation (*30*). For example, MDA-MB-231 cells carry a K-Ras mutation (*31*). In previous studies, mutant Ras isoforms cause a depletion of tropomyosin 2.1 possibly through the up-regulation of miR-21 (*32*). In terms of other ways of transforming cells, Cos7 is an SV40 transformed cell line. SV40 transformation in MEF cells increases Tpm 3 but not Tpm 2.1 expression levels (*33*). As we show here, overexpression of Tpm 3 decreases the number of CUs by competing with Tpm 2.1. Thus, classical ways of transformation normally alter different cytoskeletal protein expression levels and therefore cause depletion of CUs. This further supports the relationship between rigidity sensing CU formation and cell transformation.

An additional connection between cancer and the local CUs comes from the role that tyrosine kinases play in rigidity sensing. Previous studies show that rigidity sensing requires the action of the Src family kinases (SFKs). Knocking out the upstream activator, RPTPα, or the three Src kinases, Src, Yes, and Fyn (SYF cells) blocks the ability of those cells to sense substrate rigidity and also enables growth on soft surfaces (*34, 35*). This is consistent with our recent study that showed that ErbB family members (EGFR and HER2) are recruited to adhesion sites by SFKs on rigid surfaces and are needed for formation of CUs in early cell spreading (*6*). These findings

indicate that RTKs involved in cancer and EMT also play important roles in rigidity sensing regulation.

It is clear from many different studies that transformed cell growth is insufficient for metastasis and extensive cancer growth. However, the faulty mechanosensing machinery in transformed cells enables them to escape from the apoptosis pathways and to survive in many different environments, which is important for metastasis. Re-introduction of the missing CU components in transformed cell lines successfully rebuilds the rigidity sensing process in many different cell backgrounds. Restoring the ability to correctly sense rigidity causes transformed cells to die on soft surfaces without further manipulations. This provides a different view of blocking transformed growth. Namely, a functional rigidity sensor activates apoptosis pathways on soft surfaces and the depletion of those sensors is often sufficient for cell growth. Although there may be other mechanisms for causing growth on compliant matrices, the loss of the rigidity-sensing modules is a robust mechanism. As modular sensory units in self-driving cars are needed to stop them when an object is in their path, the modular rigidity-sensing units are needed for cells to know when the matrix is soft and growth should stop. The observation that depleting various components of rigidity-sensing modules depletes rigidity-sensing indicates that like many complex sensory modules, the rigidity-sensing contractile units require many different proteins. It is easy, therefore, to understand how many different mutations or alterations of cells could result in transformation by the loss of a critical sensory machine and why cancer is such a difficult disease to treat.

Material and Methods:

Cell culture and transfection:

HFF cells (ATCC), Cos7 cells (ATCC), MDA-MB-231 cells (gift from Dr. Jay Groves, MBI, NUS), SKOV3 cells (gift from Dr. Ruby Huang, CSI, NUS), LLC cells (ATCC) were cultured in DMEM with high glucose supplemented with 10% FBS and 1mM sodium pyruvate. HT1080 cells (ATCC) were cultured in MEM medium. Cells were transfected with DNA plasmids using lipofectamine 2000 (Invitrogen) or by Neon electroporator system (Life Technologies) according to the manufacturer's instructions. Expression vectors encoding the following fluorescent fusion proteins were used: Tpm2.1-YFP, Tpm 3-EGFP (gifts from Dr. Peter Gunning), MyosinIIA-EGFP and Emerald-myosin-IIB (gift from Dr. Michael W. Davidson group).

Transfection of siRNA and immunoblotting:

Cells were seeded into a 6-well dish on day 0 and transfected with 25 μM myosin-IIA siRNA (Dharmacon), Tpm 2.1 siRNA (Qiagen) or Tpm 3 siRNA (Dharmacon) using lipofectamine RNAiMAX (Invitrogen) on day 1. Control cells were transfected with scrambled control siRNA (Dharmacon). Transfected cells were lysed in RIPA buffer (Sigma) and proteins extracted were separated by 4-20% SDS-polyacrylamide gel (Bio-rad) and transferred to PVDF membranes (Bio-rad) at 75V for 2 hours. Membranes incubated with appropriate primary antibodies at 4°C overnight: anti-myosin-IIA (Sigma, dilution 1:1000), anti-Tpm2.1 (Abcam, dilution 1:1000), anti-TM311 (Sigma, dilution 1:1000), anti-TM γ9d (gift from Dr. Peter Gunning, dilution 1:1000), anti-EGFR (CST, dilution 1:1000), anti-HER2 (CST, dilution 1:1000), anti-ROR2 (CST, dilution 1:1000) and anti-α-tubulin (Sigma, dilution 1:3000). The primary antibody binding was processed

for ECL detection (Thermo Fisher Scientific) with appropriate HRP-conjugated secondary antibodies (Bio-rad).

Pillar fabrication, video microscopy and force traction measurements:

Molds for making PDMS pillars were fabricated as described before (*6*). 0.1g of PDMS (mixed at 10:1, Sylgard 184; Dow Corning) was poured onto the silicon mold and then flipped onto a plasma-cleaned glass bottom dish (ibdi). The sample was pressed by an 8g weight, cured at 80°C for 3 hours to reach a Young's modulus of 2MPa and was de-molded while immersed in 99.5% isopropanol. Pillars were washed with PBS for 5 times before coating with 10 µg/ml fibronectin (Roche) for cell seeding. Time-lapse imaging and traction force measurements were performed as explained before (*5*).

PAA gel preparation:

Glass bottom dishes (Iwaki) were silanizated using 1.2% 3-methacryloxypropyltrimethoxysilane (Shin-Etsu Chemical, Tokyo, Japan) in 100% Methanol for 1 hour at room temperature. 2.3 kPa Acrylamide gel was prepared as described before (*36*). Gel surfaces were treated with sulfo-SANPAN (Thermo Fisher Scientific) and exposed under UV for 5mins before coating with 10 µg/ml fibronectin for cell culture.

Fluorescence microscopy:

Cells were fixed with 4% paraformaldehyde in PBS at 37°C for 15mins and permeabilized with 0.2% TX-100 for 10 mins at room temperature. Samples were blocked with 1% bovine serum albumin (BSA) in PBS for 1h, incubated with primary antibodies for paxillin (BD, 1:200) or

Cleaved-Caspase-3 (CST, 1:200) at 4 °C overnight and then incubated with secondary antibodies (Molecular Probes) for 1h at room temperature. Fluorescence images were acquired using a spinning-disc confocal microscope (PerkinElmer Ultraview VoX) attached to an Olympus IX81 inverted microscope body.

Soft agar assay:

The soft agar assay was performed using the Cell Transformation Assays, Standard Soft Agar Kits from Cell Biolabs according to manufacturer's instructions.

Statistical analysis:

Prism (GraphPad Software) and Matlab (Math Works) were used for data analysis and graph plotting. Analyses of significant difference levels were carried out using ANOVA test (for more than 2 experimental groups) or Student's t-test.

Acknowledgements:

We thank all the members of Sheetz lab and Bershadsky lab for their kind help. This research was supported by funding to the MBI, National University of Singapore. B.Y was supported by NUS grant "Activation of Apotosis by Soft Surfaces" (R-714-000-112-133). H.W. is a David and Inez Myers Career Advancement Chair in Life Sciences fellow. M. P. S is supported by NIH grants, NUS grants and Mechanobiology Institute, National University of Singapore.

Author Contributions:

B.Y and N.N performed the experiments; S.L wrote Matlab codes for data analysis; B.Y analyzed the data; J.H provided fabrication molds; B.Y. H.W. and M.P.S wrote and prepared the manuscript.

Figure Legends:

Figure 1 Transformed cells lack rigidity sensing.

(A and B) Average number of CUs per 10 minutes generated by HFF or various transformed cell lines on rigid (k=8.4 pN/nm) and soft (k=1.6 pN/nm) pillars, respectively. (B) Staining for actin (red) and paxillin (green) in HFFs and other transformed cells on hard (2MPa) and soft (5kPa) PDMS surfaces after 6 hrs plating. (C and D) Mean single focal adhesion (FA) area (C) and cell aspect ratio (D) of HFF and various transformed cells after 6 hours plating on soft (red) and rigid (blue) PDMS surfaces. (E and F) Soft agar assay showing growth of various transformed cells but not HFF cells after 7 days culturing. Cell proliferation rate was analyzed by measuring CyQuant intensity. (Error bars are SEM. Experiments were repeated >3 times. *** stands for $p<0.001$; ** stands for $p<0.01$; * stands for $p<0.05$)

Figure 2 Transformed cells show altered expression of various mechanosensitive proteins.

(A)A structure cartoon of a typical rigidity sensing contractile unit (CU) in HFF cells. (B) Western blots of the expression levels of different mechanosensitive components in HFF and different transformed cell lines. (C) Protein expression heat map summary of various mechanosensitive proteins in various transformed cell lines.

Figure 3 Re-introduction of the missing mechanosensing cytoskeletal components restored rigidity sensing contractions.

(A and B) No contractile units were observed in wild type Cos7 cells (Cos7-WT) on both rigid (k=8.4 pN/nm) (A) and soft (k=1.6 pN/nm) (B) submicron pillars during spreading. (C and D) Myosin IIA transfected Cos7 cells (Cos7-IIA) generated contractile units (CUs) during initial

spreading on both rigid (C) and soft (D) submicron pillars. (E) Paxillin images of Cos7 cells (left panel) or EGFP-myosin IIA transfected Cos7 cells (right panel) fixed at 6 hours following seeding on rigid (2 MPa) or soft (5 kPa) fibronectin-coated PDMS surface. (F) Mean single focal adhesion (FA) area of Cos7 and Cos7-IIA cells on rigid (blue) and soft (red) PDMS surface. (G) Cartoon model summarizing findings (Error bars are SEM. >200 focal adhesions from >5 cells were analyzed in each condition. *** stands for $p<0.001$; ** stands for $p<0.01$; * stands for $p<0.05$)

Figure 4 Reciprocal depletion of mechanosensing components destroyed cell rigidity sensing process and reversed the transform phenotype.

(A) Western Blot showing Tpm 2.1 levels in Cos7 cells treated with scramble or anti-Tpm 2.1 siRNA. (B) Box-and-whisker plots of the pillars' maximum displacement values (D_{max}) by Cos7-WT, Cos7-IIA and Tpm-siRNA-transfected Cos7-IIA cells on rigid (blue) and soft (red) pillars. Silencing Tpm 2.1 in Cos7-IIA cells increased the average force level on both rigid and soft pillars. (C) Bar graphs of average number of CUs per cell per 10 minutes in Cos7-WT, Cos7-IIA and Tpm 2.1–siRNA-transfected Cos7-IIA cells on rigid (blue) and soft (red) pillars. (D and E) Soft agar assay indicating the growth of Cos7 and Tpm 2.1-knockdown Cos-7 IIA cells but not Cos7-IIA cells after 7-days of culture. (F) Western Blot showing myosin IIA levels in MDA-MB-231 cells treated with scramble or anti-myosin IIA siRNA. (G) Box-and whisker plots of Dmax of 231-WT, 231-Tpm and myosin-IIA-transfected 231-Tpm cells on rigid (blue) and soft (red) pillars. (H) Bar graphs of average of CUs per cell per 10 minutes in different cells. (I and J) Soft agar assay showing growth of MDA-MB-231 and Myosin-IIA-silenced 231-Tpm cells after 7-days of culture. (K) Cartoon model summarizing results.

Figure 5 Abnormal expression level of Tpm 3 affects cell rigidity sensing.

(A)Western blot showing Tpm 3 levels in HT1080 cells treated with scramble or anti-Tpm 3 siRNA. (B) Average number of CUs per 10 min for control and Tpm 3 depleted HT1080 cells on two pillar substrates of different rigidities. (C) Western blot showing Tpm 3 levels in MDA-MB-231 cells treated with scramble or anti-Tpm 3 siRNA. (D) Average number of CUs per 10 mins for control and Tpm 3 silenced MDA-MB-231 cells on two pillar substrates of different rigidities. (E) Soft agar assay showing growth of control HT1080 cells but not of Tpm 3 depleted or cells treated with Tpm 3 inhibitors (TR100 and ATM 3507). (F) Cartoon model summarizing results. (G) Box-and-whisker plots of the pillars' maximum displacement values (D_{max}) generated by control HFF cells and EGFP-Tpm 3 transfected HFF cells on rigid (blue) and soft (red) pillars. (H) Average number of CUs per 10 min in control and EGFP-Tpm 3 transfected HFF cells on two pillar substrates of different rigidities. (I) Cartoon model summarizing results.

Figure 6 Cartoon model summarizing findings

Supplementary Figure 1 (A) A typical example of rigidity sensing contractile unit (CU) formed by HFF cells during initial spreading (first 30 mins) on rigid pillars (k=8.4 pN/nm). (Red vectors stand for pillar displacements; Green vectors highlight CUs tracked by analysis software; Yellow line stands for cell edge).

Supplementary Figure 2 (A) Bright field images of Cos7-WT and Cos7-IIA cells growing in soft agar after 7 days.

Supplementary Figure 3 (A) Myosin-IIB and paxillin images of Cos7 cells transfected with Emerald-myosin-IIB (Cos7-IIB) on soft and rigid PDMS surfaces. (B) Bar graphs of the mean values of focal adhesion areas of Cos7-IIB cells on rigid and soft surfaces (Error bars are SEM. >200 focal adhesions from >5 cells were analyzed in each condition).

Supplementary Figure 4 (A) Box-and-whisker plots of the pillars' maximum displacement values (D_{max}) by MD-MB-231 (231-WT) and Tpm 2.1-YFP transfected MDA-MB-231 (231-Tpm) cells on rigid (blue) and soft (red) pillars. (B) Average number of CUs per 10 minutes generated by 231-WT or 231-Tpm cells on pillars with different rigidities. (C) Paxillin images of MDA-MB-231 cells (left panel) or YFP-Tpm 2.1 transfected MDA-MB-231 cells (right panel) fixed at 6 hours following seeding on rigid (2 MPa) or soft (5 kPa) fibronectin-coated PDMS surface. (D) Mean single focal adhesion (FA) area of 231-WT and 231-Tpm cells after 6 hours plating on soft (red) and rigid (blue) PDMS surfaces (Error bars are SEM. >200 focal adhesions from >5 cells were analyzed in each condition). (E) Bright field images of 231-WT and 231-Tpm cells growing in soft agar after 7 days.

Supplementary Figure 5 (A and B) Myosin IIA and paxillin images of Cos7-IIA (A) or Tpm 2.1 knockdown Cos7-IIA (B) cells spread on glass after 6 hours. (C) Mean single focal adhesion (FA) area of cells in different conditions (Error bars are SEM; >200 focal adhesions from >5 cells were analyzed in each case). (D) Caspase-3 and DAPI staining images of Cos7-WT, Cos7-IIA and Tpm 2.1 depleted Cos7-IIA cells after 3 days culturing on 2.3 kPa fibronectin coated PAA gel surfaces. (E) Average Caspase-3 intensity level measurements of cells in different conditions (Error bars are SEM; >30 cells were analyzed in each case).

Supplementary Figure 6 (A and B) Tpm 2.1 and paxillin images of 231-Tpm (A) or myosin IIA knockdown 231-Tpm (B) cells spread on glass after 6 hours. (C) Bar graphs of the mean values of focal adhesion areas of cells in different conditions (Error bars are SEM. >200 focal adhesions from >5 cells were analyzed in each condition). (D) Caspase-3 and DAPI staining images of 231-WT, 231-Tpm and myosin IIA depleted 231-Tpm cells after 3 days culturing on 2.3 kPa fibronectin coated PAA gel surfaces. (E) Average Caspase-3 intensity level measurements of cells in different conditions (Error bars are SEM; >30 cells were analyzed in each case).

Supplementary Figure 7 (A) Fluorescence images of EGFP-Tpm 3 and endogenous Tpm 2.1 in HFF cells spreading on rigid pillar surfaces. (B) Average endogenous Tpm 2.1 intensity near cell periphery in control and Tpm 3 overexpressed HFF cells. (C) Average total endogenous Tpm 2.1 intensity in control and Tpm 3 overexpressed HFF cells. (D) Cell aspect ratio of control and Tpm 3 overexpressed HFF cells after 15 mins spreading on rigid pillar surfaces.

Reference:

1. A. W. Hamburger, S. E. Salmon, Primary bioassay of human tumor stem cells. *Science* **197**, 461-463 (1977).
2. H. Wolfenson *et al.*, Tropomyosin controls sarcomere-like contractions for rigidity sensing and suppressing growth on soft matrices. *Nat Cell Biol* **18**, 33-42 (2016).
3. H. T. McMahon, E. Boucrot, Molecular mechanism and physiological functions of clathrin-mediated endocytosis. *Nature reviews. Molecular cell biology* **12**, 517-533 (2011).
4. S. Ghassemi *et al.*, Cells test substrate rigidity by local contractions on submicrometer pillars. *Proceedings of the National Academy of Sciences of the United States of America* **109**, 5328-5333 (2012).
5. B. Yang *et al.*, Mechanosensing Controlled Directly by Tyrosine Kinases. *Nano letters* **16**, 5951-5961 (2016).
6. M. Saxena *et al.*, EGFR and HER2 activate rigidity sensing only on rigid matrices. *Nat Mater* **advance online publication**, (2017).
7. G. Meacci *et al.*, α-actinin links ECM rigidity sensing contractile units with periodic cell edge retractions. *Molecular biology of the cell*, (2016).
8. D. A. Fletcher, R. D. Mullins, Cell mechanics and the cytoskeleton. *Nature* **463**, 485-492 (2010).
9. C. M. Fife, J. A. McCarroll, M. Kavallaris, Movers and shakers: cell cytoskeleton in cancer metastasis. *British Journal of Pharmacology* **171**, 5507-5523 (2014).
10. D. Schramek *et al.*, Direct in Vivo RNAi Screen Unveils Myosin IIa as a Tumor Suppressor of Squamous Cell Carcinomas. *Science* **343**, 309-313 (2014).
11. G. N. Raval *et al.*, Loss of expression of tropomyosin-1, a novel class II tumor suppressor that induces anoikis, in primary breast tumors. *Oncogene* **22**, 6194-6203 (2003).
12. J. R. Stehn *et al.*, A novel class of anticancer compounds targets the actin cytoskeleton in tumor cells. *Cancer Res* **73**, 5169-5182 (2013).
13. V. H. Freedman, S. I. Shin, Cellular tumorigenicity in nude mice: correlation with cell growth in semi-solid medium. *Cell* **3**, 355-359 (1974).
14. A. Hollestelle, F. Elstrodt, J. H. Nagel, W. W. Kallemeijn, M. Schutte, Phosphatidylinositol-3-OH kinase or RAS pathway mutations in human breast cancer cell lines. *Molecular cancer research : MCR* **5**, 195-201 (2007).
15. S. Rasheed, W. A. Nelson-Rees, E. M. Toth, P. Arnstein, M. B. Gardner, Characterization of a newly derived human sarcoma cell line (HT-1080). *Cancer* **33**, 1027-1033 (1974).
16. J. Fogh, J. M. Fogh, T. Orfeo, One hundred and twenty-seven cultured human tumor cell lines producing tumors in nude mice. *Journal of the National Cancer Institute* **59**, 221-226 (1977).
17. J. G. Mayo, Biologic characterization of the subcutaneously implanted Lewis lung tumor. *Cancer chemotherapy reports. Part 2* **3**, 325-330 (1972).
18. M. Prager-Khoutorsky *et al.*, Fibroblast polarization is a matrix-rigidity-dependent process controlled by focal adhesion mechanosensing. *Nature cell biology* **13**, 1457-1465 (2011).

19. D. M. Helfman, P. Flynn, P. Khan, A. Saeed, Tropomyosin as a regulator of cancer cell transformation. *Adv Exp Med Biol* **644**, 124-131 (2008).
20. B. Bhattacharya, G. L. Prasad, E. M. Valverius, D. S. Salomon, H. L. Cooper, Tropomyosins of human mammary epithelial cells: consistent defects of expression in mammary carcinoma cell lines. *Cancer Res.* **50**, 2105-2112 (1990).
21. M. Hendricks, H. Weintraub, Tropomyosin is decreased in transformed cells. *Proc. Natl. Acad. Sci. USA* **78**, 5633-5637 (1981).
22. V. Shah, R. Braverman, G. L. Prasad, Suppression of neoplastic transformation and regulation of cytoskeleton by tropomyosins. *Somat Cell Mol Genet* **24**, 273-280 (1998).
23. A. Masuda *et al.*, Role of a signal transduction pathway which controls disassembly of microfilament bundles and suppression of high-molecular-weight tropomyosin expression in oncogenic transformation of NRK cells. *Oncogene* **12**, 2081-2088 (1996).
24. S. Zhu, M. L. Si, H. Wu, Y. Y. Mo, MicroRNA-21 targets the tumor suppressor gene tropomyosin 1 (TPM1). *J. Biol. Chem.* **282**, 14328-14336 (2007).
25. M. L. Si *et al.*, miR-21-mediated tumor growth. *Oncogene* **26**, 2799-2803 (2006).
26. X. Zhou *et al.*, Reduction of miR-21 induces glioma cell apoptosis via activating caspase 9 and 3. *Oncology reports* **24**, 195-201 (2010).
27. J. Menez *et al.*, Mutant alpha-actinin-4 promotes tumorigenicity and regulates cell motility of a human lung carcinoma. *Oncogene* **23**, 2630-2639 (2004).
28. S. N. Nikolopoulos *et al.*, The human non-muscle alpha-actinin protein encoded by the ACTN4 gene suppresses tumorigenicity of human neuroblastoma cells. *Oncogene* **19**, 380-386 (2000).
29. P. Gunning, G. O'Neill, E. Hardeman, Tropomyosin-based regulation of the actin cytoskeleton in time and space. *Physiological reviews* **88**, 1-35 (2008).
30. T. Yamamoto, S. Taya, K. Kaibuchi, Ras-induced transformation and signaling pathway. *Journal of biochemistry* **126**, 799-803 (1999).
31. C. Scholl *et al.*, Synthetic lethal interaction between oncogenic KRAS dependency and STK33 suppression in human cancer cells. *Cell* **137**, 821-834 (2009).
32. D. Frezzetti *et al.*, Upregulation of miR-21 by Ras in vivo and its role in tumor growth. *Oncogene* **30**, 275-286 (2011).
33. J. D. Coombes *et al.*, Ras Transformation Overrides a Proliferation Defect Induced by Tpm3.1 Knockout. *Cellular & molecular biology letters* **20**, 626-646 (2015).
34. G. Jiang, A. H. Huang, Y. Cai, M. Tanase, M. P. Sheetz, Rigidity sensing at the leading edge through alphavbeta3 integrins and RPTPalpha. *Biophysical journal* **90**, 1804-1809 (2006).
35. Y. Sawada *et al.*, Force sensing by mechanical extension of the Src family kinase substrate p130Cas. *Cell* **127**, 1015-1026 (2006).
36. N. Nakazawa, A. R. Sathe, G. V. Shivashankar, M. P. Sheetz, Matrix mechanics controls FHL2 movement to the nucleus to activate p21 expression. *Proceedings of the National Academy of Sciences of the United States of America* **113**, E6813-e6822 (2016).

Cell Line Name	Resource	Anchorage-Independent Growth	Notes
HFF	Primary Human Fibroblast Cells	No	
Cos7	Monkey Kidney Fibroblast Cells	Yes	SV 40 Transformed
MDA-MB-231	Human Breast Cancer Cells	Yes	K-Ras mutated
HT1080	Human Fibrosarcoma	Yes	N-Ras mutated
SKOV3	Human Ovarian Cancer Cells	Yes	P53 mutated
LLC	Mouse Lewis Lung Carcinoma	Yes	

Table 1

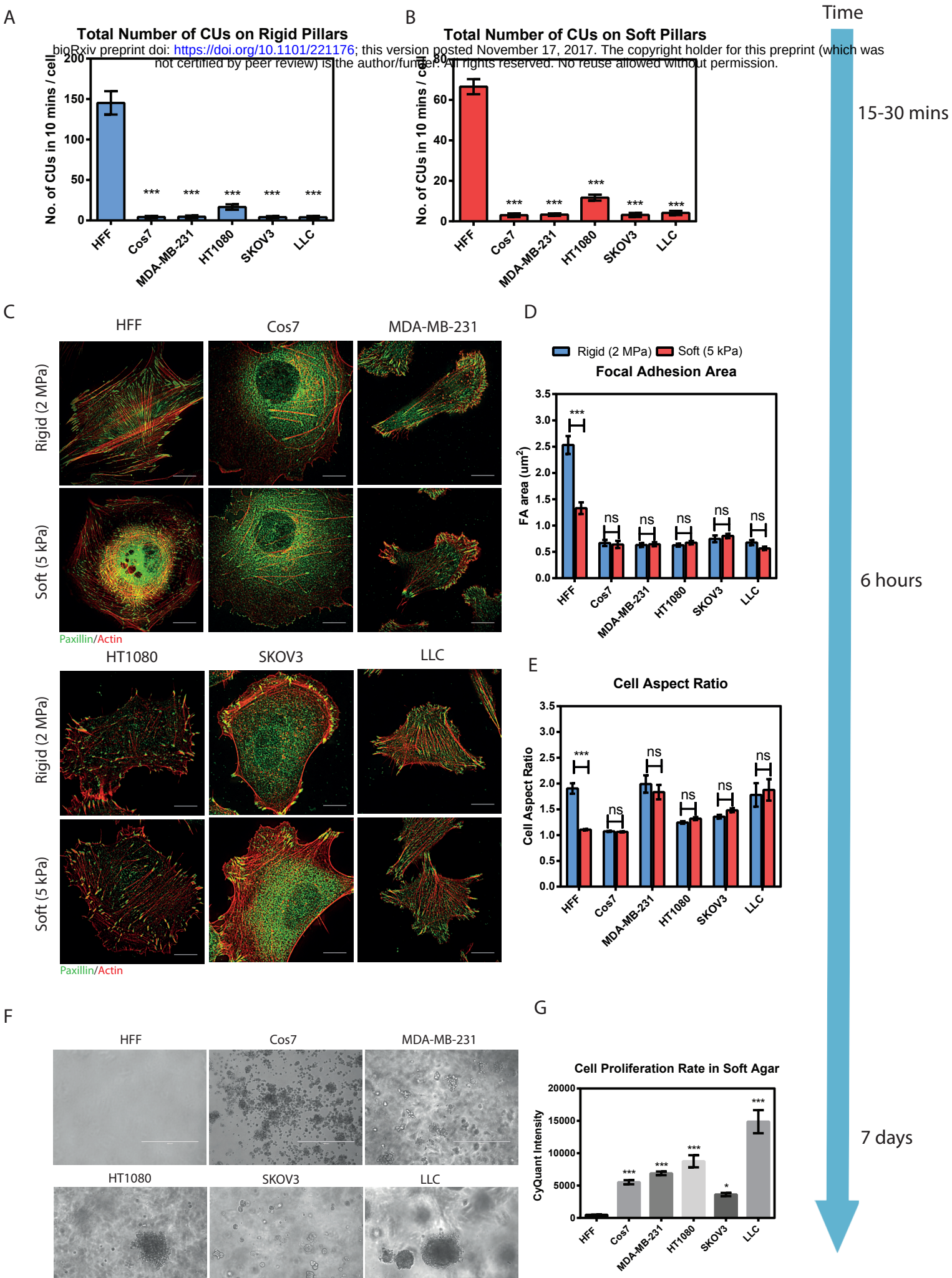

Figure 1

A

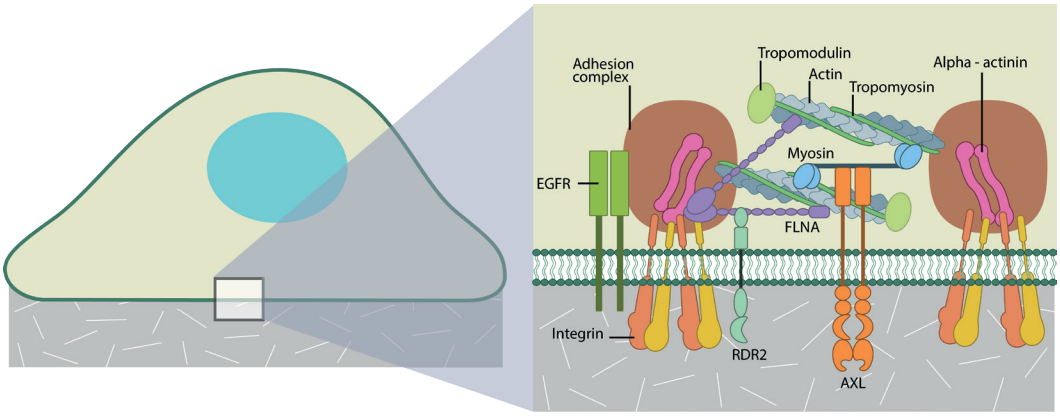

B

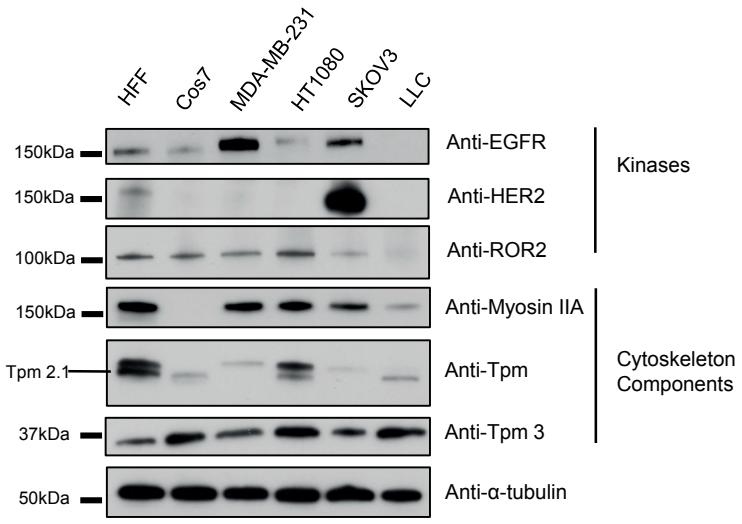

C

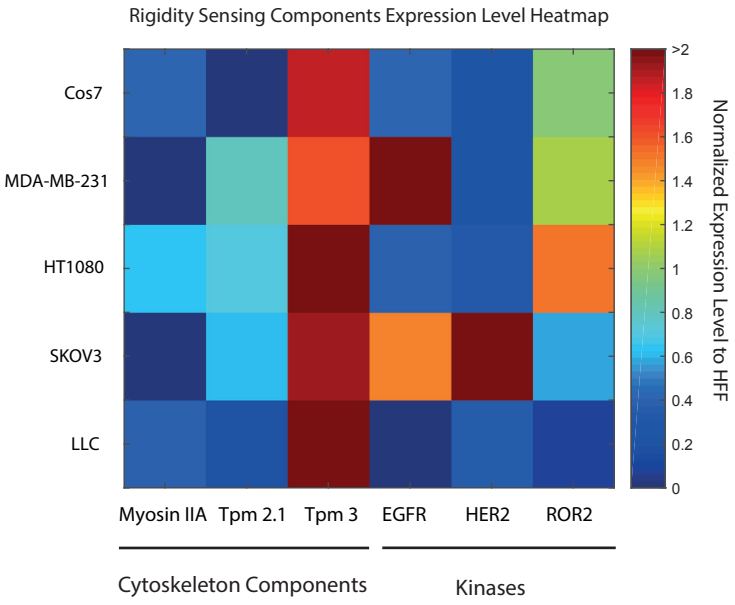

Figure 2

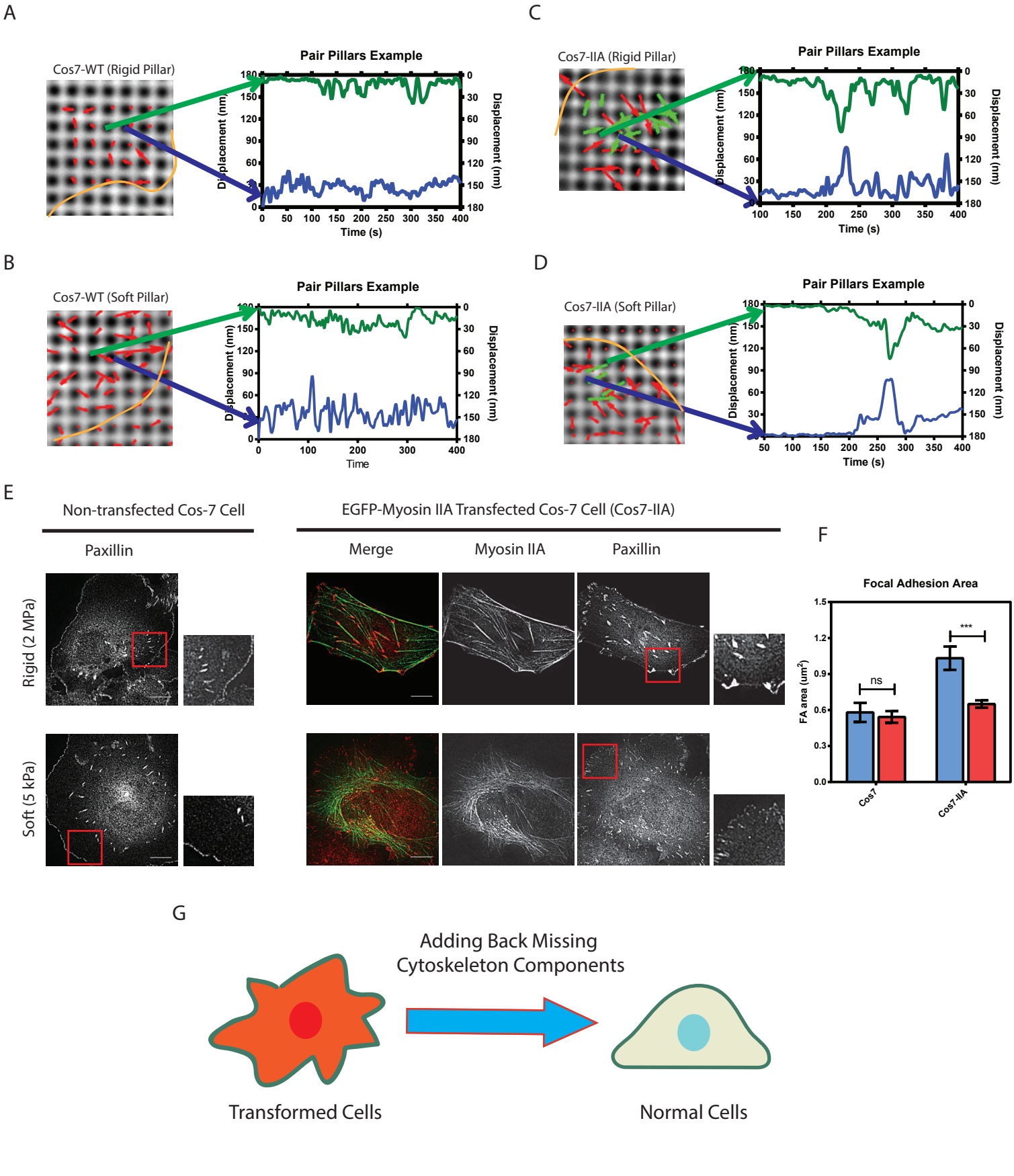

Figure 3

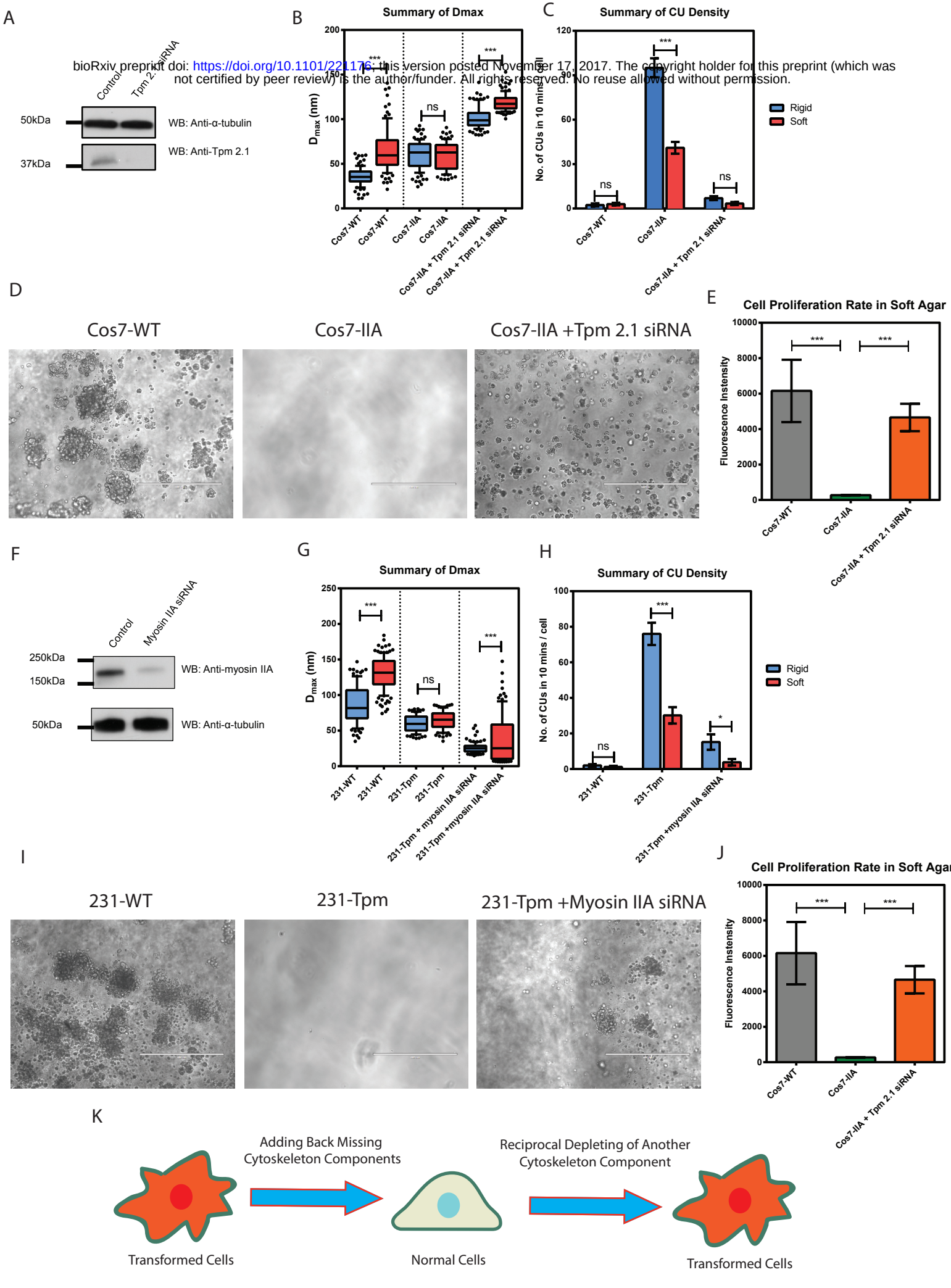

Figure 4

A

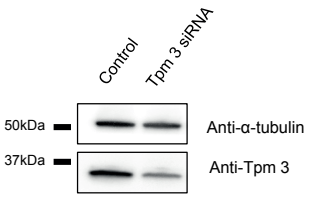

B

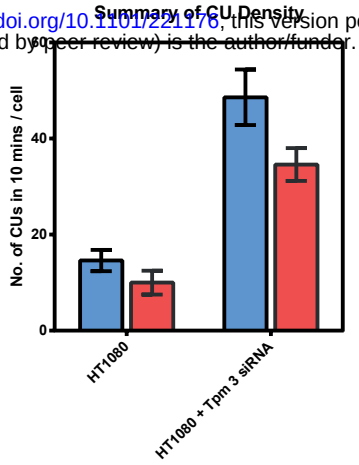

C

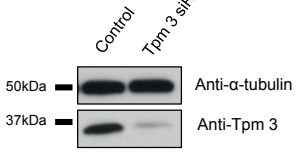

D

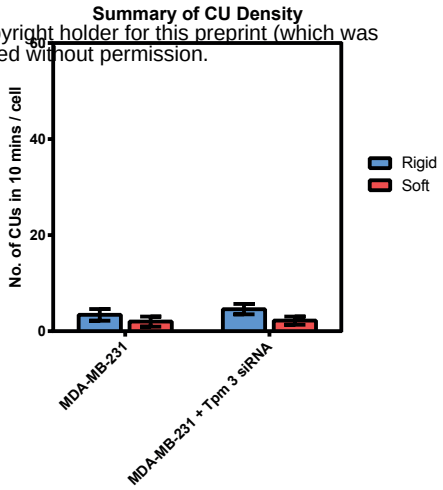

E

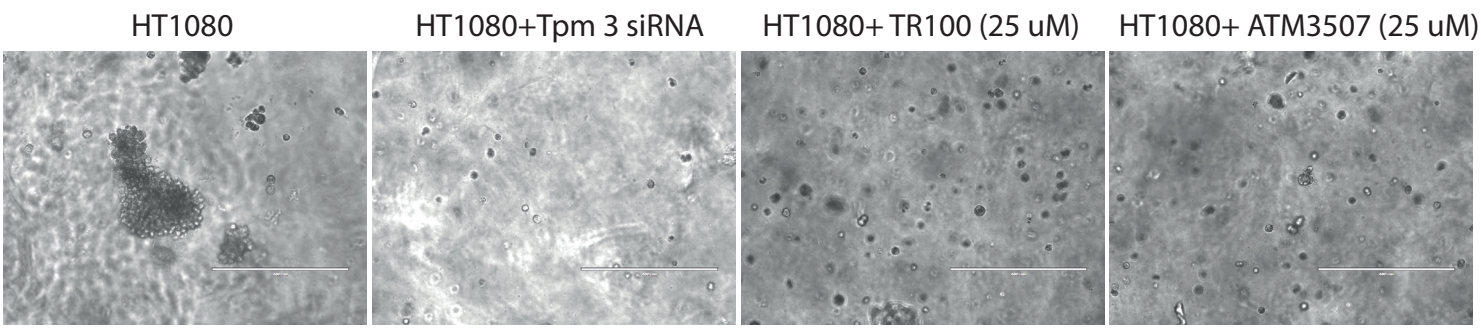

F

G

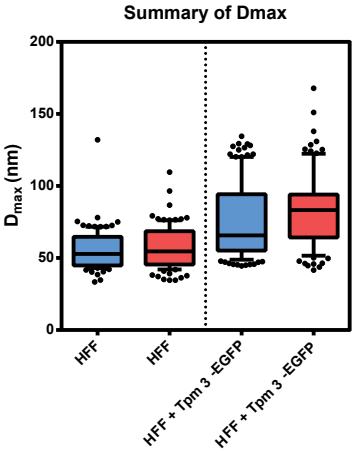

H

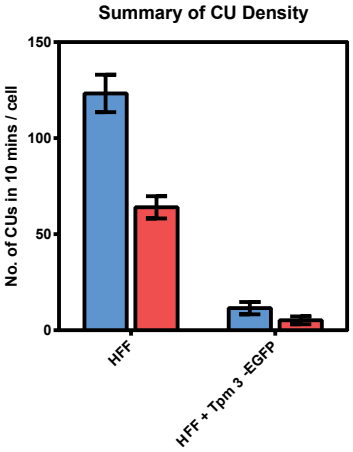

I

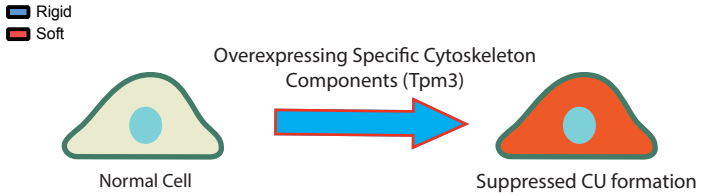

Figure 5

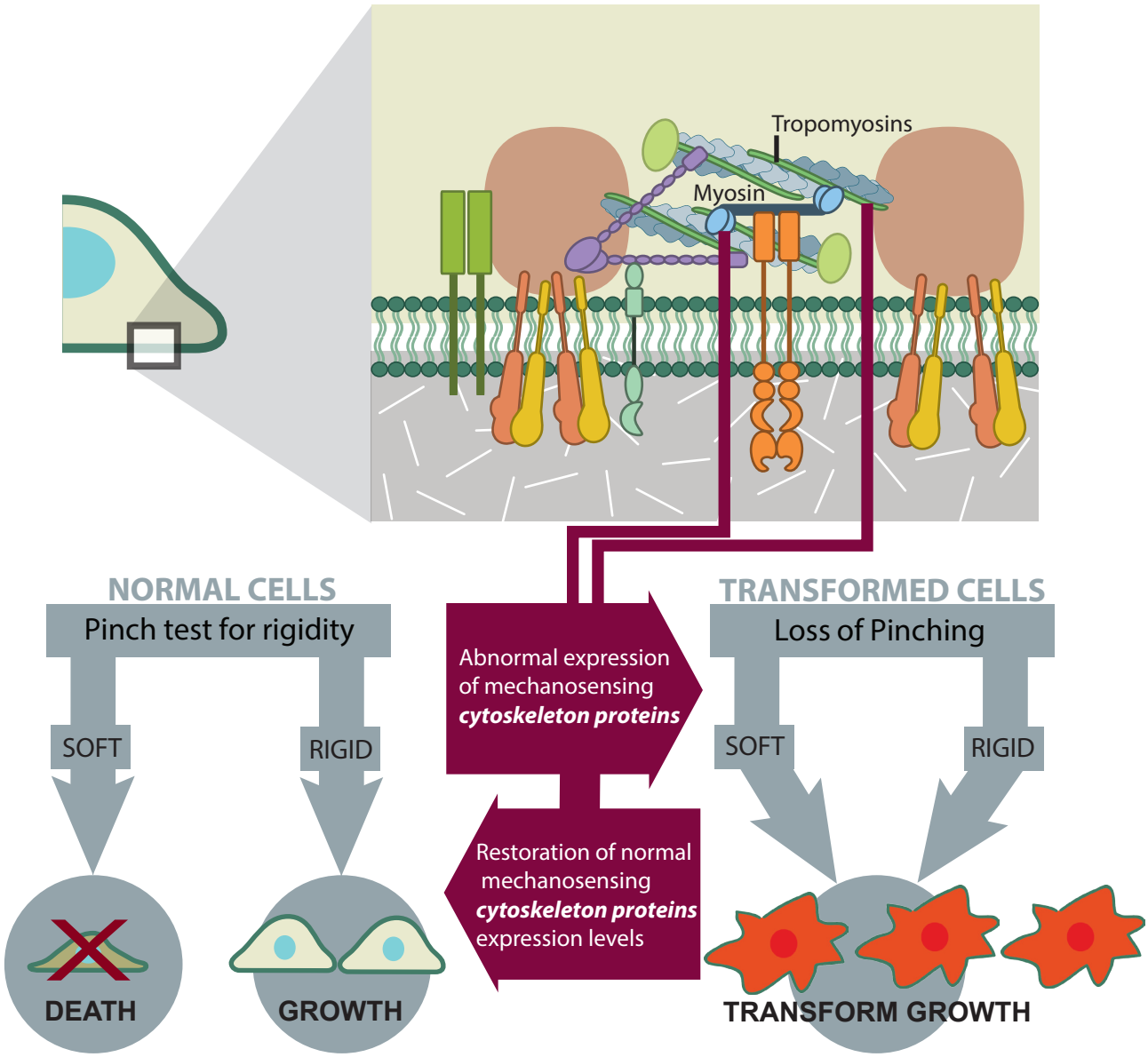

Figure 6